Int. J. Nanosci. Nanotechnol., Vol. 17, No. 4, Dec. 2021, pp. 249-260

Antibacterial Characteristics of CuS Nanoplates Anchored onto g-C_3N_4 Nanosheets, Suspended in PMMA Matrix

Akbar Mirzaei[1], Reza Peymanfar[2,*], Shahrzad Javanshir[1], Reza Fallahi[2] and Javad Karimi[2]

[1]Heterocyclic Chemistry Research Laboratory, Department of Chemistry, Iran University of Science and Technology, Tehran 16846-13114, Iran
[2]Department of Chemical Engineering, Energy Institute of Higher Education, Saveh 67746–39177, Iran

(*) Corresponding authors: reza_peymanfar@alumni.iust.ac.ir
(Received: 21 April 2021 and Accepted: 21 September 2021)

Abstract:

Nowadays, due to bacterial antibiotic resistance, the design of new high-performance antibiotics to maintain human health has been a significant challenge. Accordingly, photothermal antibiotics have been developed based on semiconductor materials such as graphene. Herein, copper sulfide (CuS) nanoplates and graphitic carbon nitride (g-C_3N_4)/CuS were synthesized as salient antibacterial agents and their antibacterial features were assessed using polymethyl methacrylate (PMMA) as a practical matrix. The morphology and structure of nanostructures were characterized by X-ray diffraction (XRD), ultraviolet (UV)-visible (Vis) diffuse reflectance spectroscopy (DRS), and field emission scanning electron microscopy (FESEM). Based on the results obtained by the UV-Vis light absorption, the g-C_3N_4, CuS, and g-C_3N_4/CuS nanostructures illustrated strong absorptions in the visible light region while demonstrated 2.92, 1.20, and 0.27 eV band gaps, respectively. Eventually, the study of the antibacterial properties of the nanostructures exhibited that the zone of inhibition is augmented by anchoring the CuS nanoplates onto the g-C_3N_4 surface. Interestingly, g-C_3N_4/CuS nanocomposite brought 12 and 17 mm zone of inhibitions for Escherichia coli (E. coli) and Staphylococcus aureus (S. aureus), respectively. More significantly, the results attested that inserting the g-C_3N_4 nanostructures promote the antibacterial features of CuS nanoplates, originated from its nucleation effect boosting surface area to volume ratio of the sulfides, amplifying interfacial interaction, and elevating established reactive oxidative species (ROS) killing the bacteria. The presented research opens new windows toward augmenting the antibacterial features of biomedical polymers.

Keyword: *Antibacterial agent, CuS nanoplates, Graphitic carbon nitride (g-C_3N_4), Polymethyl methacrylate (PMMA), Nanocomposite, Optical performance*.

1. INTRODUCTION

The bacterial infection is threatening the health of humans and any living species, on the other hand, the infecting bacteria pollute the water, soil, and the environment, eventually leading to the death of animals and plants. Therefore, till now, antibacterial agents have attracted a great deal of attentions and many of them have been developed [1]. The excessive use of antibiotics has resisted the bacteria against their drugs, causing a serious public health problem[2]. Among them, metal-based composites and semiconductor materials have recently obtained more attention [3-6]. Till date, the antibacterial properties of various metals, metal oxides, and metal sulphides consisting silver [7, 8], gold [9, 10], copper [11, 12], carrollite [13], cadmium oxide[14], cadmium hydroxide

[14], and zinc oxide [15, 16] have been evaluated. All in all, the metallic structures have exposed a significant antimicrobial activity [17-20] tuned by the shape [21], morphology [22, 23], zeta potential [24, 25], dispersion, size, and surface area to volume ratio [26, 27], etc. The antibacterial property of nanoparticles is improved by increasing the specific surface area to volume ratio [28]. Previous studies have reported that as the agglomeration of metal nanoparticles decreases, the antibacterial property is improved, even at low concentrations [29]. It should be noted that the microorganisms do not have any resistance against the metallic particles which this issue testifies to the importance of the metallic antibacterial agents. CuS is a p-type semiconductor which has recently received huge attentions due to its diverse applications in solar cells[30], photocatalysis [31], sensors [32], optical applications [33], antibacterial structures [34], and so on. Moreover, widespread morphologies of CuS nanoparticles such as nanotube [35], nanorod [36-38], nanoribbon [39] have been reported, architected using the hydrothermal and sonochemistry methods [29, 40-42]. The considerable antibacterial activity of CuS nanoparticle is mainly generated through the production of ROS [43-45]. Also, the combination of polymer and inorganic nanoparticles is attractive because g-C_3N_4 acts as a nucleation center enhancing the heterogeneous interfaces of CuS nanoparticles, desirable for antibacterial features. Interestingly, loading the nanoparticles in the polymer matrix modifies the surface of nanoparticles [46]. In this study, PMMA has been chosen as a polymeric medium due to its usability in different fields such as biomedical, energy, electronic, and optical [47]. It is well known that PMMA is one of the best choices in medical applications including contact lenses, intraocular lenses, bones, artificial corneas, artificial organs, dialysis membranes, dental materials, and so on [48, 49]. More importantly, accompanying the antibacterial characteristics develop biomedical applications of PMMA. Chitosan-g-poly(acrylamide)/CuS nano-composite has been successfully prepared for antibacterial activity against *E. coli* using microwave irradiation [50]. Also, antibacterial properties of CuS/alginate composite showed evident antibacterial activity against the *E. coli* and *L. monocytogenes* bacteria [51]. Furthermore, g-C_3N_4 with a bandgap value of 2.7 eV has become one of the extremely exciting materials due to its photocatalytic properties and antibacterial activities [52-54].

Current researches have shown that g-C_3N_4-based materials have proper antibacterial activity associated with the production of a wide variety of ROS and facile displacement of electrons in their conduction band [54-56]. Ding *et al.* have reported the preparation of CuS/protonated g-C_3N_4 composite by electrostatic bonding between protonated g-C_3N_4 and CuS [57]. The achieved results manifest in which the CuS content is 20%, the composite has synergistic effects of both photothermal and photocatalytic action under light irradiation, so antibacterial activity against *S. aureus* and *E. coli* was enhanced, attributed to the established ROS [57].

The microwave absorbing character-istics of g-C_3N_4/CuS/PMMA were reported by our researching group [58]. In this study, the antibacterial properties of g-C_3N_4, CuS, and g-C_3N_4/CuS dispersed in PMMA as a practical matrix were investigated. Herein, for the first time, the antibacterial properties of the CuS nanoplates anchored onto g-C_3N_4 nanosheets were scrupulously evaluated; giving an incomparable prospect toward augmenting the antibacterial features in the medical polymers. The result revealed the

significant antibacterial activity of CuS/PMMA and g-C_3N_4/CuS/PMMA nanocomposites against *E. coli* and *S. aureus* derived from the produced ROS.

2. EXPERIMEBTAL STEPS

2. 1. Material

All chemicals used in this study were analytical grade and were used without further treatment. Sodium sulfide hydrate (60.0-62.0%) was obtained from Samchun Chemicals (South Korea) while copper (II) acetate (OAc) monohydrate, urea, and dichloromethane (DCM) were purchased from Merck (Germany). PMMA as a polymeric medium was obtained from Sigma-Aldrich (United States America). Bacteria including *E. coli* PTCC 1330 and *S. aureus* 25935 were purchased from Persian type culture collection, an Iranian research organization for science and technology (IROST).

2. 2. Synthesis of g-C_3N_4

The g-C_3N_4 structure was fabricated by the methods reported in previous researches [59, 60]. For the synthesis of g-C_3N_4, urea (15 g) was dissolved in 20 mL water and then dried at 50˚C for 24 h. In the next step, the dried urea was heated in a furnace for 5 h at 520 °C.

2. 3. Preparation of CuS Nanoplates

CuS nanoplates were prepared using a hydrothermal method [61]. In a typical synthesis, Cu $(OAc)_2$. H_2O (1.8 g) was dissolved in deionized water (30 mL) and added to an aqueous solution of sodium sulfide hydrate (1.76 g). The solution was transferred into a 100 mL Teflon-lined stainless steel autoclave and heated at 180 ˚C for 18 h. After being cooled to room temperature, the resulting solid was centrifuged, washed with deionized water and anhydrous ethanol, and dried at 50 ˚C for 6 h.

2. 4. Preparation of g-C_3N_4/CuS Nano-composite

The g-C_3N_4/CuS nanocomposite was obtained by a complementary sono-chemical and hydrothermal method [59]. The g-C_3N_4 (20 wt. % of CuS nanoplate) was added to a water/ethanol (65 wt. %) solution. Afterward, Cu $(OAc)_2$. H_2O (0.7 g) was added and the suspension was treated by ultrasound waves for 30 min. Then, a solution of sodium sulfide (1.8 g in 30 mL water) was slowly added to the aforementioned suspension under ultrasound waves. Finally, the suspension was sonicated for 30 min and annealed at 180 °C for 18 h. The tailored precipitate was rinsed and dried at 50 °C.

2. 5. Molding the Samples Using PMMA Matrix

Each sample (50 wt. %) was dispersed in PMMA solution (40 wt. % in DCM) by ultrasound waves for 20 min. Eventually, the nanocomposites were obtained by drying the suspensions at 60 °C. Fig.1 illustrates a schematic representation of the experimental scenarios applied to prepare the nanostructures [58].

2. 6. Antibacterial Activity

Antibacterial activity of g-C_3N_4, CuS nanoplate, and g-C_3N_4/CuS nanocomposite was performed using the diffusion method in Mueller-Hinton agar. Briefly, a suspension (0.5×10^8 CFU/mL) of *E. coli* and *S. aureus* bacteria was spread on an agar culture medium**.**

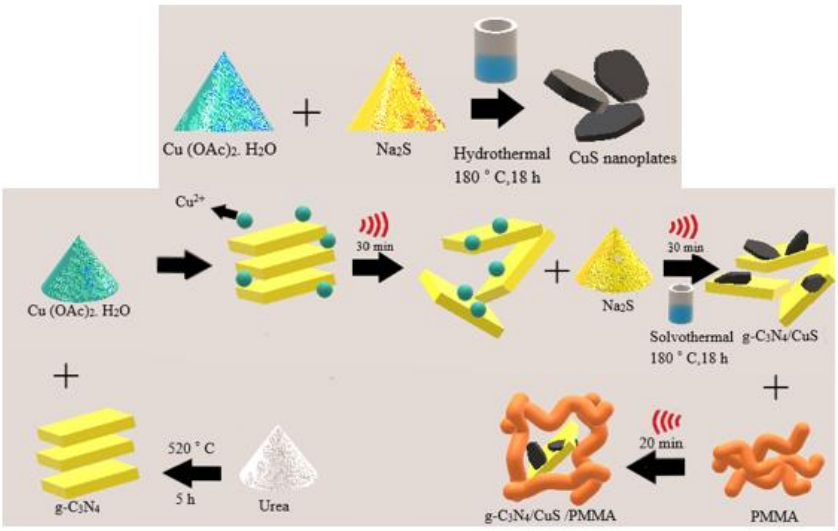

Figure1. *Schematic representation of the experimental scenarios.*

Then, g-C_3N_4/PMMA, CuS nanoplate/ PMMA, and g-C_3N_4/CuS/PMMA (13 mg) were placed in the culture media and incubated at 37 ° C for 24 h [62, 63]. Vancomycin and streptomycin as positive and negative control were applied, respectively.

3. RESULTS AND DISCUSSION

3. 1. Field Emission Scanning Electron Microscopy (FESEM) Micrographs

The morphology of g-C_3N_4, CuS nanoplate, and g-C_3N_4/CuS nanocomposite was investigated by FESEM micrographs (Fig. 2a-d). As can be seen, the shapeless g-C_3N_4 (Fig. 2a) was obtained using urea as a precursor. The results show that the preparation of CuS by hydrothermal method leads to the hexagonal morphology of CuS (Fig. 2b, c). FESEM images of g-C_3N_4/CuS (Fig. 2d, e) indicated a uniform distribution of hexagonal CuS nanostructures onto the shapeless g-C_3N_4 structures, prepared in water/ethanol solvent by a sonochemical and solvothermal complementary method.

3. 2. XRD Patterns

Fig. 3 shows the XRD patterns of g-C_3N_4, CuS, and g-C_3N_4/CuS nanocomposite. As displayed in the patterns, the peaks existing at 2θ= 26.79◦, 27.32◦, 28.87◦, 31.39◦, 32.42◦, 47.21◦, 47.41◦, 52.20◦, 59.01◦ correspond respectively to (100), (101), (102), (103), (006), (107), (110), (108), (116) crystal planes confirming that the crystalline phase of hexagonal CuS was formed, based on JCPDS card number: [01-078-0876]. According to the Sherrer equation, the particle size of CuS nanoplates is 10.3 nm [58, 64].

XRD pattern of g-C_3N_4/CuS also confirms that the crystalline structure of CuS nanoplates has been maintained after the applied experimental scenario. The g-C_3N_4 is synthesized by conjugated tri-s-triazine unit and the peaks at 2θ= 13.12◦ and 27.50◦ related to (100) and (200) crystal planes confirm its formation, given by JCPDS number of [01–087-1526] [58, 65-67]. It should be noted that the intensity of g-C_3N_4 peaks in g-C_3N_4/CuS is negligible due to the more mass fraction and intense crystalline structure of CuS. On the other hand, the used high-power ultrasound waves expand the stacked g-C_3N_4 leading to the exfoliation of polymeric layers and elevating its amorphous structure [58, 68-70].

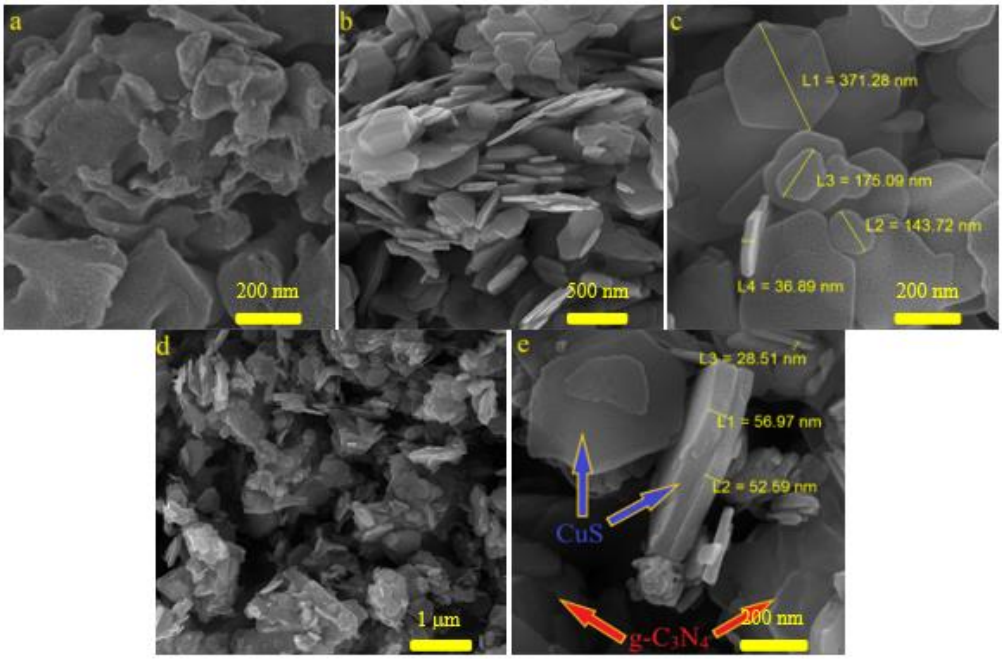

Figure 2. *FESEM micrographs of g-C_3N_4 (a), CuS nanoplates (b, c), and g-C_3N_4/CuS nanocomposite (d, e).*

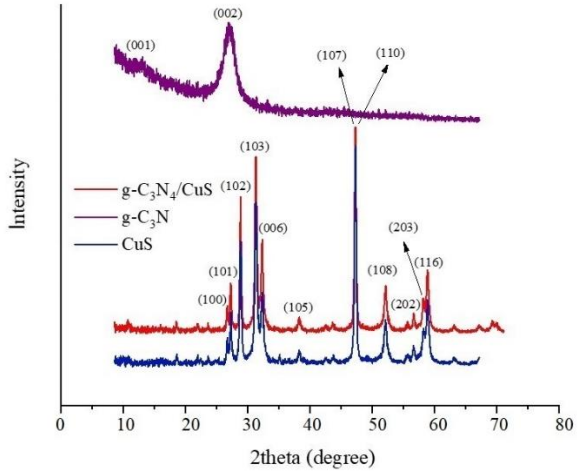

Figure 3. *XRD patterns of g-C_3N_4, CuS, and g-C_3N_4/CuS nanostructures.*

3. 3. FTIR of the Samples

The chemical functional groups of g-C_3N_4, CuS, and CuS/g-C_3N_4 nanostructures were investigated by FTIR spectroscopy (Fig. 4). The broadband peak observed at 1250-1600 cm^{-1} is related to the C-N and C=N stretching vibrations of the tri-s-triazine rings. Furthermore, the presence of triazine units is approved by the sharp absorption band at 860 cm^{-1} [67, 70]. Besides, the peaks ascribed to the amino groups of g-C_3N_4 were obtained at 3175 cm^{-1}. Noticeably, the diminution of g-C_3N_4 peaks in the synthesized CuS/g-C_3N_4 composite is due to the high content of CuS [58].

The stretching vibration band of Cu-S and Cu=S were observed at 421 and 611 cm^{-1}, respectively. The peak at 1097 cm^{-1} was attributed to S-Cu-S [27, 29]. The assigned broadband peak around 3450 cm^{-1} corresponds to the stretching mode of the hydroxyl groups and the notch at 1630 cm^{-1} is associated with the bending mode of H–O–H of the adsorbed water [71]. The peak at 2356 cm^{-1} arises from the adsorbed CO_2 [70].

3. 4. UV-Vis Spectra

According to the UV-Vis spectra, g-C_3N_4, CuS, and g-C_3N_4/CuS showed strong absorption in the visible light region (Fig. 5a, b).

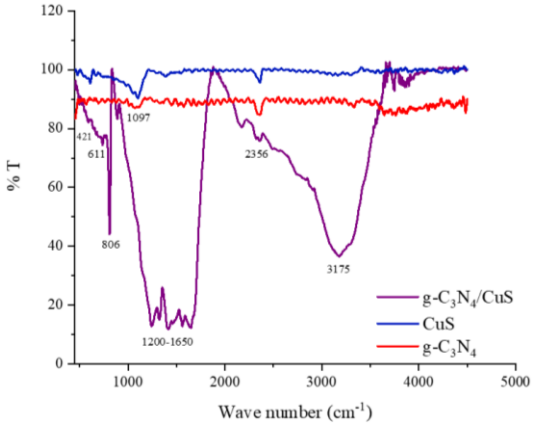

Figure 4. *FT-IR spectra of g-C_3N_4, CuS, and g-C_3N_4/CuS nanostructures.*

Obviously, ornamenting the g-C_3N_4 by CuS nanostructures increased the absorption intensity. Recently, similar results have been reported for the UV-Vis absorption of g-C_3N_4/CuS composites (Fig. 5a)[72, 73]. The bandgap energy (BGE) and UV–Vis absorption properties of g-C_3N_4, CuS, and g-C_3N_4/CuS nanostructures were characterized as shown in Fig. 5a, b. UV–Vis absorption occurs by charge transfer from the valance band to the conduction band. The BGE for g-C_3N_4, CuS, and g-C_3N_4/CuS was calculated using Kubelka-Munk theory [74]. Results have shown that BGE of g-C_3N_4, CuS, and g-C_3N_4/CuS were 2.92, 1.20, and 0.27 eV, respectively (Fig. 5b). Based on the BGE results, g-C_3N_4 exhibited a semiconductor feature which is due to the intra and intermolecular electronic transitions from n and π→π* in the conjugated structures[75]. Also, d→d transmissions of CuS nanoplates promote the light adsorption in the g-C_3N_4/CuS nanocomposite [58]. Considering the morphological effect on the BGE, CuS has shown a narrower BGE than previous research (1.70–1.96 eV) [76].

3. 5. Antibacterial Activity

Previous researches have shown that g-C_3N_4 and CuS, under visible light radiation, form ROS by transferring electrons from the valance band to the conduction band [54-56].

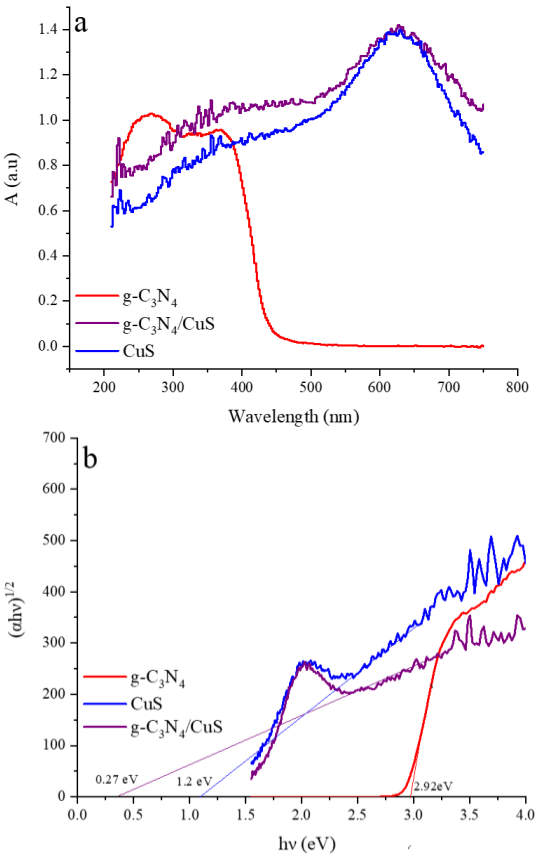

Figure 5. *UV−Vis DRS (a) and $(\alpha hv)^{1/2}$ vs. hv plots (b) of g-C_3N_4, CuS, and g-C_3N_4/CuS nanostructures.*

Herein, the antibacterial properties of g-C_3N_4, CuS, and g-C_3N_4/CuS nanostructures were studied without visible light radiation. The antibacterial test did not show any antibacterial activity for g-C_3N_4 but CuS and g-C_3N_4/CuS demonstrated significant antibacterial features (Table.1). Fig. 6a, b show the antibacterial assays of g-C_3N_4, CuS, and g-C_3N_4/CuS nanostructures against *E. coli* and *S. aureus*. The recent reports have indicated that the antibacterial activity of CuS nanoparticles depends on the type of bacteria due to their different cell wall structures [51, 77].

Generally, diverse mechanisms have been proposed to antibacterial properties of CuS

nanoparticles. It is believed that free Cu^{2+} produced by CuS destroys the cell wall through interaction with the negatively charged membrane protein. It has also been reported that the proximity of CuS nanoparticles with bacterial cells can cause wrinkles and damage to the bacterial wall [43]. Another plausible interpretation is ROS produced by CuS nanoparticles. Oxidative stress by ROS is one of the most striking antibacterial mechanisms of nanoparticles [78-80]. Particularly, the aerobic respiration of bacteria reduces molecular oxygen and produce O_2^- and H_2O_2 [81]. Not only CuS have substantial photocatalytic activity but also has a Fenton-like catalyst activity. Noticeably, Cus degrades a wide range of microorganisms without light radiation. Fenton reaction leads to the production of ROS, following that the established ROS including free radical species-mediated ($OH^{\cdot}$ and $O_2^{\cdot -}$) leads to cell death through damaging the cell membranes [43, 51, 82-85]. As indicated, g-C_3N_4/CuS has a more inhibitory effect on all bacteria than CuS. Based on Ayodhya *et al.* research, increasing the surface area of CuS enhances the antibacterial activity [86]. The dispersion of nanoparticles is highly affected by the inorganic nanoparticle-polymer interaction and compatibility. For incompatible systems, the separation of nanoparticle occurs through a dominant erosion process while for compatible systems, the size of the nanoparticles is decreased by rapid and efficient disruption. It has been shown that the dispersion of CuS nanoparticles onto the g-C_3N_4 structures as well as the distribution of the filler in a system containing PMMA matrix can be increased [46, 87]. The electrostatic interactions play a vital role in paving the way for the proper dispersion of the nanostructures, enhancing antibacterial characteristics. More significantly, the FESEM micrographs testify that CuS nanoplates are dispersed on the g-C_3N_4 interfaces. As a result, the heterogeneous interfaces of g-C_3N_4 act as nucleation centers enhancing the surface area to volume ratio of the nanoparticles by enhancing their dispersion and diminishing their average size. It should be noted that the ultrasound waves reinforce the dispersion of the nanoparticles, tune their size, and expand the stacked polymers [88, 89]. It can be seen that the antibacterial activity is related to the surface area and dispersion of nanoparticles. Thus, increasing the distribution of CuS nanoplates onto the g-C_3N_4 surface amplifies the antibacterial activity of g-C_3N_4/CuS nanocomposite (Fig. 6a, b). Interestingly, PMMA composites demonstrated proper antibacterial characteristics desirable for practical applications in the biomedical fields. Fig. 6c, d illustrates a negative and positive control using streptomycin and vancomycin to more correlate the achieved results.

Table1. *Comparing the bacterial zone of growth inhibition.*

Sample	Zone of inhibition (mm)	
	E. coli	*S. aureus*
g-C_3N_4/PMMA	-	-
CuS/PMMA	10	10
g-C_3N_4/CuS/PMMA	12	17
control	23	20

4. CONCLUSION

In summary, g-C_3N_4, CuS, and g-C_3N_4/CuS nanostructures were fabricated using simple scenarios by annealing, hydrothermal, and sonochemical method. The architected structures were blended by PMMA as a practical medium. The UV-Vis spectra demonstrated that the g-C_3N_4/CuS nanocomposite could absorb both UV and visible light.

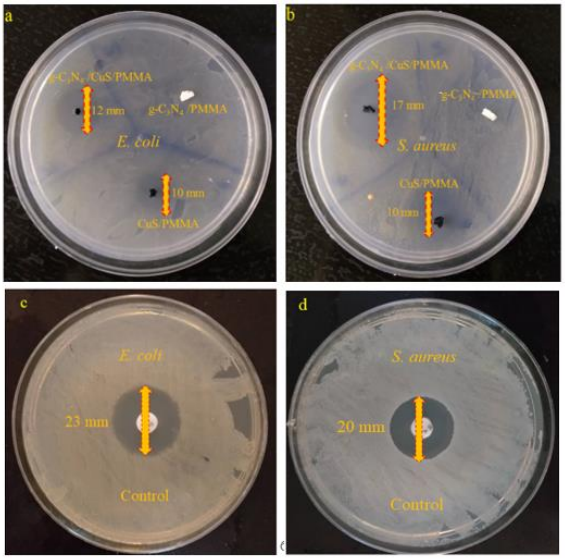

Figure 6. *Antibacterial activity of g-C_3N_4/PMMA, CuS/PMMA, and g-C_3N_4/CuS/PMMA against E. coli (a), S. aureus (b), negative control (c), and positive control (d).*

Nevertheless, the antibacterial properties investigated against gram-positive and negative bacteria (*S. aureus* and *E. coli*) were performed without light radiation. The FESEM images indicated that CuS nanoplates are well dispersed onto the g-C_3N_4 interfaces.The achieved results declared that g-C_3N_4/CuS nanocomposite has significant antibacterial activity due to the modified structure of CuS anchored onto the g-C_3N_4. The diameters of inhibition zones against *E. coli* and *S. aureus* were 12 and 17 mm for g-C_3N_4/CuS/PMMA, respectively. Therefore, CuS and g-C_3N_4/CuS nanostructures can be applied as practical antibacterial filler to establish antibacterial feature in PMMA. The presented research suggests an incomparable prospect to augment the antibacterial characteristics in the biomedical polymers.

ACKNOWLEDGEMENT

The authors wish to express their gratitude for the financial support provided by the Research Council of Iran University of Science and Technology (IUST), Tehran, Iran.

CONFLICT OF INTEREST

The authors declare that they have no conflict of interest.

REFERENCES

1. Breijyeh, Z., Jubeh, B., Karaman, R., ‘‘Resistance of Gram-negative bacteria to current antibacterial agents and approaches to resolve it’’, *Molecules*, 25 (2020) 1340.
2. Thapa, S. P., Shrestha, S., & Anal, A. K., ‘‘Addressing the antibiotic resistance and improving the food safety in food supply chain (farm-to-fork) in Southeast Asia’’, *Food Control*, 108 (2020) 106809.
3. Talebian, N., Nilforoushan, M. R., & Zargar, E. B., ‘‘Enhanced antibacterial performance of hybrid semiconductor nanomaterials: ZnO/SnO2 nanocomposite thin films’’, *Applied Surface Science*, 258 (2011). 547-555.
4. Wang, L., Zhang, X., Yu, X., Gao, F., Shen, Z., Zhang, X., Chen, C., ‘‘An all organic semiconductor C3N4/PDINH heterostructure with advanced antibacterial photocatalytic therapy activity’’, *Advanced Materials*, 31 (2019) 1901965.
5. Pant, B., Pant, H. R., Barakat, N. A., Park, M., Jeon, K., Choi, Y., Kim, H. Y., ‘’Carbon nanofibers decorated with binary semiconductor (TiO2/ZnO) nanocomposites for the effective removal of organic pollutants and the enhancement of antibacterial activities’’, *Ceramics International*, 39 (2013) 7029-7035.
6. Aksoy, I., Kucukkececi, H., Sevgi, F., Metin, O., & Hatay Patir, I., ‘‘Photothermal antibacterial and antibiofilm activity of black phosphorus/gold nanocomposites against pathogenic bacteria’’, *ACS Applied Materials & Interfaces*, 12 (2020) 26822-26831.
7. John, T., Parmar, K. A., Kotval, S. C., & Jadhav, J., ‘‘Synthesis, Characterization, Antibacterial and Anticancer Properties of Silver Nanoparticles Synthesized from Carica Papaya Peel Extract’’, *International Journal of Nanoscience and Nanotechnology*, 17 (2021) 23-32.

8. Waghmode, S. R., Dudhane, A. A., & Mhaindarkar, V. P., ‘‘Syzygium cumini Mediated Green Synthesis of Silver Nanoparticles for Reduction of 4-Nitrophenol and Assessment of its Antibacterial Activity’’, (2021).
9. Hussein, M. A. M., Grinholc, M., Dena, A. S. A., El-Sherbiny, I. M., & Megahed, M., ‘‘Boosting the antibacterial activity of chitosan–gold nanoparticles against antibiotic–resistant bacteria by Punicagranatum L. extract’’,*Carbohydrate Polymers*, 256 (2021) 117498.
10. Dudhane, A. A., Waghmode, S. R., Dama, L. B., Mhaindarkar, V. P., Sonawane, A., & Katariya, S., ‘‘Synthesis and Characterization of Gold Nanoparticles using Plant Extract of Terminalia arjuna with Antibacterial Activity’’, *International Journal of Nanoscience and Nanotechnology*, 15 (2019) 75-82.
11. Guo, G., Xu, Q., Zhu, C., Yu, J., Wang, Q., Tang, J., ... & Zhang, X., ‘‘Dual-temporal bidirectional immunomodulation of Cu-Zn Bi-layer nanofibrous membranes for sequentially enhancing antibacterial activity and osteogenesis’’, *Applied Materials Today*, 22 (2021) 100888.
12. Jose, M., Szymańska, K., Szymański, K., Moszyński, D., Mozia, S,‘‘Effect of copper salts on the characteristics and antibacterial activity of Cu-modified titanate nanotubes’’, *Journal of Environmental Chemical Engineering*, 8 (2020) 104550.
13. Peymanfar, R., Selseleh-Zakerin, E., Ahmadi, A., Tavassoli, S. H., ‘‘Architecting functionalized carbon microtube/carrollite nanocomposite demonstrating significant microwave characteristics’’, *Scientific reports*, 11 (2021) 1-15.
14. Mirzaei, A., Jamshidi, E., Morshedloo, E., Javanshir, S., & Manteghi, F., ‘‘Carrageenan assisted synthesis of morphological diversity of CdO and Cd (OH) 2 with high antibacterial activity’’, *Materials Research Express*, 8 (2021) 065006.
15. Aquisman, A. E., Wee, B. S., Chin, S. F., Kwabena, D. E., Michael, K. O., Bakeh, T., Sylvester, D. S., ‘‘Synthesis, Characterization, and Antibacterial Activity of ZnO Nanoparticles from Organic Extract of Cola Nitida and Cola Acuminata Leaf’’, *International Journal of Nanoscience and Nanotechnology*, 16 (2020) 73-89.
16. Pal, S., Mondal, S., Maity, J., Mukherjee, R., ‘‘Synthesis and characterization of ZnO nanoparticles using Moringa oleifera leaf extract: investigation of photocatalytic and antibacterial activity’’, *International Journal of Nanoscience and Nanotechnology*, 14 (2018) 111-119.
17. Wang, B., Moon, J. R., Ryu, S., Park, K. D., Kim, J. H., ‘‘Antibacterial 3D graphene composite gel with polyaspartamide and tannic acid containing in situ generated Ag nanoparticle’’, *Polymer Composites*, 41 (2020) 2578-2587.
18. Chen, J., Li, H., Fang, C., Cheng, Y., Tan, T., Han, H., ‘‘ In situ synthesis and properties of Ag NPs/carboxymethyl cellulose/starch composite films for antibacterial application’’, *Polymer Composites*, 41 (2020) 838-847.
19. Shariatinia, Z., Nikfar, Z., Gholivand, K., Abolghasemi Tarei, S., ‘‘Antibacterial activities of novel nanocomposite biofilms of chitosan/phosphoramide/Ag NPs’’, *Polymer Composites*, 36 (2015) 454-466.
20. Nahar, K., Aziz, S., Bashar, M., Haque, M., Al-Reza, S. M., ‘‘Synthesis and characterization of Silver nanoparticles from Cinnamomum tamala leaf extract and its antibacterial potential’’, *International Journal of Nano Dimension*, 11 (2020) 88-98.
21. Cheon, J. Y., Kim, S. J., Rhee, Y. H., Kwon, O. H., Park, W. H., ‘‘Shape-dependent antimicrobial activities of silver nanoparticles’’, *International journal of nanomedicine*, 14 (2019) 2773.
22. Kasi, G., Viswanathan, K., & Seo, J., Effect of annealing temperature on the morphology and antibacterial activity of Mg-doped zinc oxide nanorods’’, *Ceramics International*, 45 (2019) 3230-3238.
23. Ali, S., Perveen, S., Ali, M., Jiao, T., Sharma, A. S., Hassan, H., Chen, Q., ‘‘Bioinspired morphology-controlled silver nanoparticles for antimicrobial application’’, *Materials Science and Engineering: C*, 108 (2020) 110421.
24. Arakha, M., Saleem, M., Mallick, B. C., Jha, S., ‘‘The effects of interfacial potential on antimicrobial propensity of ZnO nanoparticle’’, *Scientific reports*, 5 (2015) 1-10.
25. Salvioni, L., Galbiati, E., Collico, V., Alessio, G., Avvakumova, S., Corsi, F., Colombo, M.,‘‘Negatively charged silver nanoparticles with potent antibacterial activity and reduced toxicity for pharmaceutical preparations’’, *International Journal of Nanomedicine*, 12 (2017) 2517.
26. Truong, T. T. V., Kumar, S. R., Huang, Y. T., Chen, D. W., Liu, Y. K., Lue, S. J., Size-Dependent Antibacterial Activity of Silver Nanoparticle-Loaded Graphene Oxide Nanosheets’’, *Nanomaterials*, 10 (2020) 1207..
27. Sirelkhatim, A., Mahmud, S., Seeni, A., Kaus, N. H. M., Ann, L. C., Bakhori, S. K. M., Mohamad, D., ‘‘Review on zinc oxide nanoparticles: antibacterial activity and toxicity mechanism’’, *Nano-micro letters*, 7 (2015) 219-242.

28. Mirzaei, A., Peymanfar, R., Khodamoradipoor, N., ‘‘Investigation of size and medium effects on antimicrobial properties by CuCr2O4 nanoparticles and silicone rubber or PVDF’’, *Materials Research Express*, 6 (2019) 085412.
29. Tian, Y., Qi, J., Zhang, W., Cai, Q., Jiang, X., Facile, one-pot synthesis, and antibacterial activity of mesoporous silica nanoparticles decorated with well-dispersed silver nanoparticles’, *ACS applied materials & interfaces*, 6 (2014) 12038-12045.
30. Xu, Z., Li, T., Zhang, F., Hong, X., Xie, S., Ye, M., Liu, X.,‘‘Highly flexible, transparent and conducting CuS-nanosheet networks for flexible quantum-dot solar cells’’, *Nanoscale*, 9 (2017).3826-3833.
31. Tirado, J., Roldán-Carmona, C., Muñoz-Guerrero, F. A., Bonilla-Arboleda, G., Ralaiarisoa, M., Grancini, G., Jaramillo, F., Copper sulfide nanoparticles as hole-transporting-material in a fully-inorganic blocking layers nip perovskite solar cells: Application and working insights’’, *Applied Surface Science*, 478 (2019) 607-614.
32. Borthakur, P., Das, M. R., Szunerits, S., Boukherroub, R.,‘‘CuS decorated functionalized reduced graphene oxide: a dual responsive nanozyme for selective detection and photoreduction of Cr (VI) in an aqueous medium’’, *ACS Sustainable Chemistry & Engineering*, 7 (2019) 16131-16143.
33. Nath, S. K., Kalita, P. K.,‘‘Temperature dependent structural, optical and electrical properties of CuS nanorods in aloe vera matrix’’, *Nano-Structures & Nano-Objects*, 25 (2021) 100651.
34. Cao, C., Wang, F., Lu, M., ‘‘Preparation of superhydrophobic CuS cotton fabric with photocatalytic and antibacterial activity for oil/water separation’’, *Materials Letters*, 260 (2020) 126956.
35. Du, C., Zhu, Y., Wang, Z., Wang, L., Younas, W., Ma, X., Cao, C., ‘‘Cuprous self-doping regulated mesoporous CuS nanotube cathode materials for rechargeable magnesium batteries’’, *ACS applied materials & interfaces*, 12 (2020) 35035-35042.
36. Guan, J., Peng, J., Jin, X., ‘‘Synthesis of copper sulfide nanorods as peroxidase mimics for the colorimetric detection of hydrogen peroxide’’, *Analytical Methods*, 7 (2015) 5454-5461.
37. Pal, D., Singh, G., Goswami, Y. C., & Kumar, V., Synthesis of randomly oriented self assembled CuS nanorods by co-precipitation route’’, *Journal of Materials Science: Materials in Electronics*, 30 (2019)15700-15704.
38. Yendrapati, T. P., Gautam, A., Bojja, S., Pal, U., ‘‘Formation of ZnO@ CuS nanorods for efficient photocatalytic hydrogen generation’’, *Solar Energy*, 196 (2020) 540-548.
39. Xu, P., Miao, C., Cheng, K., Ye, K., Yin, J., Cao, D., Zhang, X., ‘‘High electrochemical energy storage performance of controllable synthesis of nanorod Cu1. 92S accompanying nanoribbon CuS directly grown on copper foam’’, *Electrochimica Acta*, 214 (2016) 276-285.
40. ChongYeon, P. A. R. K., Ghosh, T., ZeDa, M. E. N. G., Kefayat, U., Vikram, N., WonChun, O. H.,‘‘Preparation of CuS-graphene oxide/TiO2 composites designed for high photonic effect and photocatalytic activity under visible light’’, *Chinese Journal of Catalysis*, 34 (2013) 711-717.
41. Yu, S., Liu, J., Zhu, W., Hu, Z. T., Lim, T. T., Yan, X., ‘‘Facile room-temperature synthesis of carboxylated graphene oxide-copper sulfide nanocomposite with high photodegradation and disinfection activities under solar light irradiation’’, *Scientific reports*, 5 (2015) 1-12.
42. Zhang, Y. Q., Zhang, B. P., Ge, Z. H., Zhu, L. F., Li, Y., ‘‘Preparation by solvothermal synthesis, growth mechanism, and photocatalytic performance of CuS nanopowders’’,*European Journal of Inorganic Chemistry*, (2014) 2368-2375.
43. Ahmed, K. B. A., Anbazhagan, V., ‘‘Synthesis of copper sulfide nanoparticles and evaluation of in vitro antibacterial activity and in vivo therapeutic effect in bacteria-infected zebrafish’’, *RSC advances*, 7 (2017) 36644-36652.
44. Wang, H. Y., Hua, X. W., Wu, F. G., Li, B., Liu, P., Gu, N., Chen, Z., ‘‘Synthesis of ultrastable copper sulfide nanoclusters via trapping the reaction intermediate: potential anticancer and antibacterial applications’’, *ACS applied materials & interfaces*, 7 (2015) 7082-7092.
45. N Oktar, F., Yetmez, M., Ficai, D., Ficai, A., Dumitru, F., Pica, A., ‘‘Molecular mechanism and targets of the antimicrobial activity of metal nanoparticles’’, *Current topics in medicinal chemistry*, 15 (2015) 1583-1588.
46. Šupová, M., Martynková, G. S., Barabaszová, K., ‘‘Effect of nanofillers dispersion in polymer matrices: a review’’, *Science of advanced materials*, 3 (2011) 1-25.
47. Ali, U., Karim, K. J. B. A., Buang, N. A.,‘‘A review of the properties and applications of poly (methyl methacrylate)(PMMA)’’, *Polymer Reviews*, 55 (2015) 678-705.
48. Lee, J. H., Jo, J. K., Kim, D. A., Patel, K. D., Kim, H. W., Lee, H. H., Nano-graphene oxide incorporated into PMMA resin to prevent microbial adhesion’’, *Dental Materials*, 34 (2018) e63-e72.
49. Ebnesajjad, S. (Ed.)., ‘‘*Handbook of biopolymers and biodegradable plastics: properties, processing and applications*,’’ William Andrew. (2012).

50. Pathania, D., Gupta, D., Agarwal, S., Asif, M., Gupta, V. K., ‘‘Fabrication of chitosan-g-poly (acrylamide)/CuS nanocomposite for controlled drug delivery and antibacterial activity’, *Materials Science and Engineering: C*, 64 (2016) 428-435.
51. Roy, S., Rhim, J. W., ‘‘Effect of CuS reinforcement on the mechanical, water vapor barrier, UV-light barrier, and antibacterial properties of alginate-based composite films’’, *International Journal of Biological Macromolecules*, 164 (2020) 37-44.
52. Akple, M. S., Low, J., Wageh, S., Al-Ghamdi, A. A., Yu, J., Zhang, J., ‘‘Enhanced visible light photocatalytic H2-production of g-C3N4/WS2 composite heterostructures’’, *Applied Surface Science*, 358 (2015) 196-203.
53. Nayak, S., Mohapatra, L., Parida, K., ‘‘Visible light-driven novel gC 3 N 4/NiFe-LDH composite photocatalyst with enhanced photocatalytic activity towards water oxidation and reduction reaction’’, *Journal of Materials Chemistry A*, 3 (2015) 18622-18635.
54. Lang, Q., Hu, W., Zhou, P., Huang, T., Zhong, S., Yang, L., Bai, S., ‘‘Twin defects engineered Pd cocatalyst on C3N4 nanosheets for enhanced photocatalytic performance in CO2 reduction reaction’’, *Nanotechnology*, 28 (2017) 484003.
55. Yang, Y., Zeng, Z., Zeng, G., Huang, D., Xiao, R., Zhang, C., He, D., ‘‘Ti3C2 Mxene/porous g-C3N4 interfacial Schottky junction for boosting spatial charge separation in photocatalytic H2O2 production’’, *Applied Catalysis B: Environmental*, 258 (2019) 117956.
56. Thurston, J. H., Hunter, N. M., Cornell, K. A. (2016). ‘‘Preparation and characterization of photoactive antimicrobial graphitic carbon nitride (g-C 3 N 4) films’’. *RSC advances*, 6 (48), 42240-42248..
57. Ding, H., Han, D., Han, Y., Liang, Y., Liu, X., Li, Z., Wu, S.,‘‘Visible light responsive CuS/protonated g-C_3N_4 heterostructure for rapid sterilization’’, *Journal of hazardous materials*, 393 (2020) 122423.
58. Peymanfar, R., Karimi, J., Fallahi, R., ‘‘Novel, promising, and broadband microwave absorbing nanocomposite based on the graphite like carbon nitride/CuS’’, *Journal of Applied Polymer Science*, 137 (2020) 48430.
59. Liu, X., Li, X., Shan, Y., Yin, Y., Liu, C., Lin, Z., & Kumar, S. S. (2020). ‘‘CuS nanoparticles anchored to gC 3 N 4 nanosheets for photothermal ablation of bacteria’’. *RSC Advances*, 10 (21), 12183-12191.
60. Peymanfar, R., Selseleh-Zakerin, E., Ahmadi, A., ‘‘Tailoring energy band gap and microwave absorbing features of graphite-like carbon nitride (g-C3N4)’’. *Journal of Alloys and Compounds*, 867 (2021) 159039.
61. Mezgebe, M. M., Ju, A., Wei, G., Macharia, D. K., Guang, S., Xu, H., ‘‘Structure based optical properties and catalytic activities of hydrothermally prepared CuS nanostructures’’; *Nanotechnology*, 30 (2019) 105704.
62. Díez-Pascual, A. M., Luceño-Sánchez, J. A., ‘‘Antibacterial Activity of Polymer Nanocomposites Incorporating Graphene and Its Derivatives’’: A State of Art, *Polymers*, 13 (2021) 2105.
63. Aldosari, M. A., Alsaud, K. B. B., Othman, A., Al-Hindawi, M., Faisal, N. H., Ahmed, R., Asharaeh, E., ‘‘Microwave Irradiation Synthesis and Characterization of Reduced-(Graphene Oxide-(Polystyrene-Polymethyl Methacrylate))/Silver Nanoparticle Nanocomposites and Their Anti-Microbial Activity’’, *Polymers*, 12 (2020) 1155.
64. Peymanfar, R., Ahmadi, M., Javanshir, S., ‘‘Tailoring GO/BaFe12O19/La0. 5Sr0. 5MnO3 ternary nanocomposite and investigation of its microwave characteristics’’, *Materials Research Express*, 6 (2019) 085063.
65. Jiang, L., Wang, Z., Geng, D., Wang, Y., An, J., He, J., Zhang, Z., ‘‘Carbon-encapsulated Fe nanoparticles embedded in organic polypyrrole polymer as a high performance microwave absorber’’, *The Journal of Physical Chemistry C*, 120 (2016) 28320-28329.
66. Wang, Z., Guan, W., Sun, Y., Dong, F., Zhou, Y., Ho, W. K., ‘‘Water-assisted production of honeycomb-like gC 3 N 4 with ultralong carrier lifetime and outstanding photocatalytic activity’’, *Nanoscale*, 7 (2015) 2471-2479.
67. Xia, P., Zhu, B., Yu, J., Cao, S., Jaroniec, M., ‘‘Ultra-thin nanosheet assemblies of graphitic carbon nitride for enhanced photocatalytic CO 2 reduction’’, *Journal of Materials Chemistry A*, *5* (2017) 3230-3238.
68. Peymanfar, R., Javidan, A., Javanshir, S., ‘‘Preparation and investigation of structural, magnetic, and microwave absorption properties of aluminum-doped strontium ferrite/MWCNT/polyaniline nanocomposite at KU-band frequency’’,*Journal of Applied Polymer Science*, 134 (2017) 45135.
69. Zhang, X. J., Wang, G. S., Cao, W. Q., Wei, Y. Z., Liang, J. F., Guo, L., & Cao, M. S., Enhanced microwave absorption property of reduced graphene oxide (RGO)-MnFe2O4 nanocomposites and polyvinylidene fluoride’’, *ACS applied materials & interfaces*, 6 (2014) 7471-7478.
70. Peymanfar, R., Afghahi, S. S. S., Javanshir, S., ‘‘Preparation and investigation of structural, magnetic, and microwave absorption properties of a SrAl1. 3Fe10. 7O19/multiwalled carbon nanotube nanocomposite in X and Ku-band frequencies’’, *Journal of nanoscience and nanotechnology*, 19 (2019) 3911-3918.

71. Gupta, V. K., Pathania, D., Agarwal, S., Singh, P., ‘‘Adsorptional photocatalytic degradation of methylene blue onto pectin–CuS nanocomposite under solar light’’, *Journal of Hazardous Materials*, 243 (2012) 179-186.
72. Ayodhya, D., Veerabhadram, G., ‘‘Influence of g-C3N4 and g-C3N4 nanosheets supported CuS coupled system with effect of pH on the catalytic activity of 4-NP reduction using NaBH4’’, *FlatChem*, 14 (2019) 100088.
73. Chen, W., Liu, T. Y., Huang, T., Liu, X. H., Zhu, J. W., Duan, G. R., Yang, X. J., ‘‘In situ fabrication of novel Z-scheme Bi2WO6 quantum dots/g-C3N4 ultrathin nanosheets heterostructures with improved photocatalytic activity’’, *Applied Surface Science*, *355* (2015) 379-387.
74. Wang, X., Fan, J., Qian, F., Min, Y., Magnetic BiFeO 3 grafted with MWCNT hybrids as advanced photocatalysts for removing organic contamination with a high concentration’’, *RSC advances*, *6* (2016) 49966-49972.
75. Habibi-Yangjeh, A., Mousavi, M., ‘‘Deposition of CuWO4 nanoparticles over g-C3N4/Fe3O4 nanocomposite: novel magnetic photocatalysts with drastically enhanced performance under visible-light’’, *Advanced Powder Technology*, 29 (2018) 1379-1392.
76. Tanveer, M., Cao, C., Aslam, I., Ali, Z., Idrees, F., Tahir, M., Mahmood, A., ‘‘Effect of the morphology of CuS upon the photocatalytic degradation of organic dyes’’, *RSC advances*, 4 (2014) 63447-63456.
77. Anitha, S., Brabu, B., Thiruvadigal, D. J., Gopalakrishnan, C., Natarajan, T. S., ‘‘Optical, bactericidal and water repellent properties of electrospun nano-composite membranes of cellulose acetate and ZnO’’, *Carbohydrate polymers*, 87 (2012) 1065-1072.
78. Mazur, P., Skiba-Kurek, I., Mrowiec, P., Karczewska, E., & Drożdż, R., ‘‘Synergistic ROS-associated antimicrobial activity of silver nanoparticles and gentamicin against staphylococcus epidermidis’’, *International journal of nanomedicine*, 15 (2020) 3551.
79. Barber, T. L., Aldinger, J., Arnold, J., Leonard, S., Ding, M., ‘‘Copper oxide nanoparticles activate Nrf2, KEAP 1, and downstream target genes in JB6 cells possibly through ROS generation and antioxidant response element (ARE) mechanisms’’, *The FASEB Journal*, 34 (2020) 1-1.
80. Liu, Z., Qu, X., ‘‘New insights into nanomaterials combating bacteria: ROS and beyond’’, *Science China Life Sciences*, 62 (2019) 150-152.
81. Palza, H., Antimicrobial polymers with metal nanoparticles’’. *International journal of molecular sciences*, 16 (2015) 2099-2116.
82. Ma, Y., Zhang, J., Wang, Y., Chen, Q., Feng, Z., Sun, T.,‘‘Concerted catalytic and photocatalytic degradation of organic pollutants over CuS/g-C3N4 catalysts under light and dark conditions’’, *Journal of advanced research*, 16 (2019) 135-143.
83. Deng, C., Ge, X., Hu, H., Yao, L., Han, C., Zhao, D.,‘‘Template-free and green sonochemical synthesis of hierarchically structured CuS hollow microspheres displaying excellent Fenton-like catalytic activities’’, *CrystEngComm*, 16 (2014) 2738-2745.
84. Shu, Q. W., Lan, J., Gao, M. X., Wang, J., Huang, C. Z., ‘‘Controlled synthesis of CuS caved superstructures and their application to the catalysis of organic dye degradation in the absence of light’’, *CrystEngComm*, 17 (2015) 1374-1380.
85. Nidheesh, P. V., Gandhimathi, R., Ramesh, S. T., ‘‘Degradation of dyes from aqueous solution by Fenton processes: a review’’, *Environmental Science and Pollution Research*, 20 (2013) 2099-2132.
86. Ayodhya, D., & Veerabhadram, G., ‘‘Preparation, characterization, photocatalytic, sensing and antimicrobial studies of Calotropis gigantea leaf extract capped CuS NPs by a green approach’’, *Journal of Inorganic and Organometallic Polymers and Materials*, 27 (2017) 215-230.
87. Nurul Reffa Azyan, N., Norkhairunnisa, M., Tay, C. H., Hanim, A.,‘‘Techniques on Dispersion of Nanoparticles in Polymer Matrices: A Review’’, *Pertanika Journal of Science & Technology*, 25 (2017).
88. Farazas, A., Mavropoulos, A., Christofilos, D., Tsiaousis, I., Tsipas, D., ‘‘Ultrasound assisted green synthesis and characterization of graphene oxide’’, *International Journal of Nanoscience and Nanotechnology*, 14 (2018) 11-17.
89. Jafari, V., Allahverdi, A., ‘‘Synthesis and characterization of colloidal nanosilica via an ultrasound assisted route based on alkali leaching of silica fume’’. *International Journal of Nanoscience and Nanotechnology*, 10 (2014) 145-152.

.